

Optimization of Dynamic Characteristics of Automatic-Firing Muzzle with Damping

Zhiqian Wang^{*}, Baoquan Mao, Yongliang Wu, Xianghua Bai, Shuai Feng,
Xiaoping Han, Cheng Li, and Tu Lan

Department of Weapons and Control Engineering, Army Academy of Armored Forces, Beijing, 100072, China

Abstract

In order to improve the inadequate firing accuracy of the existing prototype of a 30-mm caliber gun overhead weapon station, a triple-index constrained optimization model with damper is developed with the consideration of a real-world operating environment. Furthermore, a method of deriving the characteristic parameters of the damper is proposed based on the triple indices, and the optimal damping parameters are obtained. Simulation results show that the dynamic characteristics of the automatic-firing muzzle of the overhead weapon station with the proposed damper have been significantly improved, where the dispersion variances of horizontal and pitching are decreased by more than 30%, indicating that the firing accuracy is considerably enhanced. The result can be applied for the development of overhead weapon stations in the future.

Keywords: the overhead weapons station; optimization of dynamic characteristics of muzzle; the damping buffer device; triple-index constraints

(Submitted on September 20, 2018; Revised on October 17, 2018; Accepted on November 19, 2018)

© 2019 Totem Publisher, Inc. All rights reserved.

Nomenclatures

- ω_n ---The natural frequency of the system
 ζ ---The damping ratio
 V_0 ---The initial speed of the recoil structure
 $G(t)$ ---The impact force
 σ ---The displacement limit
 k --- The stiffness
 c --- The damping coefficient
 ω_d ---The frequency of system attenuation vibration
 $|x_w|$ ---The absolute value of system steady-state displacement
 X_{peak} ---The maximum recoil displacement
 t_w ---The steady-state time
 σ_{peak} ---The maximum steady-state displacement
 Q_1 ---The maximum acceleration
 Q_2 ---The maximum steady-state displacement
 Q_3 ---The maximum recoil displacement

* Corresponding author.
E-mail address: 980020762@qq.com

1. Introduction

Overhead weapon station (OWS) is a modular weapon system that can be equipped on multiple platforms, reduce weapon system response time, and solve the problem that operators normally do not have armor protection [1]. However, the existing weapon station commonly yields poor accuracy and dispersion, due to insufficient the damping effect provided by the recoil-attenuating device that connects the gun body and the mounting structure. Therefore, such a device is incapable of dissipating the great energy generated when the gun fires.

According to the artillery recoil device design experience, damping elements to the device can absorb recoil energy, reducing muzzle vibration. The goal of weapon station researchers is to design a new recoil-attenuating device including damping elements to improve the existing spring buffer.

Nowadays, the fast development of new buffer material, such as magneto-rheological fluid [2-3], electro-rheological fluid [4], compressible fluid [5], rubber composites [6], polymers [7-8], air spring [9], and metal rubber [10], provides a new way of designing a new recoil-attenuating device. Hence, these are used at home and abroad to control the launch of artillery and automatic weapons. For example, Ahmadian et al. [11-12] attempted to use a magneto rheological damping control system in a gun recoil system and showed that using the magneto rheological damper can control the regularity of recoil. Patil et al. [13] used a high yield strength electro-rheological fluid (ER) to design a semi-active smart recoil system for artillery guns that can improve emissivity and firing accuracy by adjusting the damping force. Chen [14] applied an elastomer buffer to the artillery recoil reducer, established an impact environmental mechanics model suitable for the elastomer buffer, and systematically studied the time-varying characteristics of the damping parameters of the elastomer buffer. Regardless of which cushioning material or combination of cushioning media is chosen, the modification of spring stiffness, damping coefficient, and damping ratio of the cushioning device is essentially involved.

Hence, based on the real-world operating requirements of the overhead weapon station, an optimal design model of the buffer device with multi-indices constraints is established in this paper. This model is used to obtain the optimal buffer device parameters and lay the ground for the future development of recoil-attenuating devices.

2. Design Specifications for the Recoil-Attenuating Device with Damping

The buffer device of the overhead weapon station is fixed to a cradle, which can absorb and release energy through deformation. The damping component within the device can dissipate part of the recoil energy, reducing the impact of the shooting load on the mounting system and thus attenuating the effect of the impact response on muzzle vibration, the sighting device, and the stabilizing system, which leads to better dispersion. The overhead weapon station usually takes automatic-firing as the main operating condition and requires the recoil part to be reset to the initial steady position in a very short time to reduce the initial disturbance when firing the next round. Meanwhile, the continuous feeding system also requires the maximum displacement of recoil to be strictly controlled within a certain range. Therefore, the design of a damping buffer device should meet the following three requirements.

2.1. Maximum Acceleration

Lightweight design of overhead weapons station requires that the dimensions of the mounting system (cradle, bracket), pitch/orientation motor size, motor power, maximum motor torque, and impact force transmitted to the mounting system are within a limit. The physical contact between components caused by the impact load and the elastic deformation of the mounting system are the most important factors that cause the muzzle vibration. In order to maintain good firing accuracy, the maximum impact force cannot be kept below a threshold. In an overhead weapon system, the sighting device is coaxially connected with the trunnion. A large impact force will cause the sight line to vibrate, affecting sighting accuracy. In the worst-case scenario, the sight sighting device can even be damaged. Therefore, the damping buffer device should be able to limit the maximum impact force, in order to meet the requirements of the permissible impact load of the mounting system and the sighting device.

The motion of an over-head weapon system with damping during recoiling is governed by the following differential equations:

$$\begin{cases} M\ddot{X} + C\dot{X} + KX = 0 \\ X(0) = 0, \dot{X}(0) = V_0 \end{cases} \quad (1)$$

The natural frequency of the system is $\omega_n = \sqrt{K/M}$, and the damping ratio is $\zeta = C/(2\sqrt{KM}) = C/(2M\omega_n)$. Thus, the above equation can be expressed as:

$$\ddot{X} + 2\zeta\omega_n\dot{X} + \omega_n^2 X = 0 \quad (2)$$

Reference [15] indicates that the velocity step technique can be used to simplify the calculation of the system impact response. Therefore, the initial speed of the recoil structure (V_0) is assumed to be equal to the maximum velocity produced after firing (v_{\max}). In other words, $V_0 \approx v_{\max}$. Assuming that $x(t) = X(t)/v_{\max}$, Equation (2) can be further written as:

$$\begin{cases} \ddot{x} + 2\zeta\omega_n\dot{x} + \omega_n^2 x = 0 \\ x(0) = 0, \dot{x}(0) = 1 \end{cases} \quad (3)$$

Figure 1 provides a free-body diagram that describes the motion of the recoil structure. The impact force is defined as:

$$G(t) = m\ddot{x}(t) = c\dot{x}(t) + kx(t) \quad (4)$$

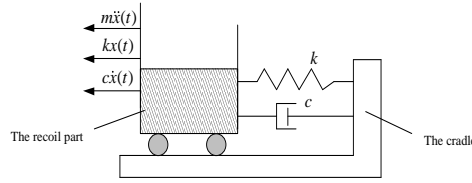


Figure 1. Free-body diagram of an overhead weapons station

According to the maximum impact requirements, $G(t) = m\ddot{x}(t)$ should be less than a certain threshold. Considering the mass of the recoil part m is a constant value, the maximum acceleration is used to meet the maximum impact requirements. The definition of the maximum acceleration of a damping buffer device is:

$$Q_1 = \max_t |\ddot{x}(t)| \quad (5)$$

2.2. Maximum Steady-State Displacement

In order to ensure the firing dispersion, an overhead weapon station is required to have better launch stability, including blowback and counter-recoil stability. In order to make sure that the recoil part can reset to the equilibrium position quickly during continuous firing, the damping buffer device needs to have quick reset.

According to the concept of steady-state displacement in [16], the steady-state displacement can be used to indicate how fast a reset process is. Therefore, the steady-state displacement in this study is defined such that: After time t_w , the maximum displacement of the system is less than the displacement limit σ , that is, the system is stable at this time. However, after time t_w , the maximum displacement is the maximum steady-state displacement. Thus, the definition of the maximum steady-state displacement indicators of the damping buffer device is:

$$Q_2 = \max_{t \geq t_w} |x(t)| \quad (6)$$

2.3. Maximum Recoil Displacement

The ammunition box of the overhead weapon station is connected to an auto-feeding mechanism by the rotary hard guidance and the flexible guidance. The excessively large recoil displacement can easily lead to poor feeding in automatic-firing. As a result, the recoil displacement must be within a certain range. Namely, the maximum displacement of the damping buffer device is less than the maximum allowable displacement of the recoil displacement. Therefore, the definition of the maximum recoil displacement of the damping buffer device is:

$$Q_3 = \max_t |x(t)| \quad (7)$$

For a recoil-attenuating device with determined initial parameters, Q_1 , Q_2 , Q_3 are functions of the natural frequency ω_n and damping ratio ζ . The system stiffness k and damping coefficient c can therefore be determined based on the natural frequency and damping ratio. Hence, the design of the damping buffer device is turned into an optimization problem to minimize the effect of the maximum acceleration Q_1 on the steady-state displacement Q_2 and the maximum recoil displacement Q_3 . The optimization model can be expressed as:

$$\begin{cases} \min_{\omega_n, \zeta} Q_1 \\ s.t. \\ Q_2 < \sigma_{peak} \\ Q_3 = X_{peak} \end{cases} \quad (8)$$

3. Impact Response Solution

The kinematic differential Equations (3) can be used to solve the acceleration response, steady-state displacement response, and recoil displacement response of the buffer system with different damping ratios. In this paper, only the response of small damping ratio ($0 \leq \zeta < 1$) is considered, and the critical damping and over damping are not analyzed.

3.1. Acceleration Response Solution

The system acceleration response can be obtained from Equation (3) [17]:

$$\ddot{x}(t) = \frac{\omega_n}{\sqrt{1-\zeta^2}} e^{-\zeta\omega_n t} \sin(\omega_d t - 2 \arctan \frac{\sqrt{1-\zeta^2}}{\zeta}) \quad (9)$$

Where $\omega_d = \omega_n \sqrt{1-\zeta^2}$ is the frequency of system attenuation vibration.

Differentiating Equation (9) and setting the time derivative equal to zero, we can determine when the maximum acceleration response happens, which gives:

$$t_a = \frac{1}{\omega_d} (3 \arctan \frac{\sqrt{1-\zeta^2}}{\zeta} + k\pi) \quad (10)$$

Since the maximum absolute value of the system acceleration response only occurs at $t = 0$ s or at the first extremum, which is affected by the phase, the time of the first extremum of the acceleration response depends on the magnitude of the damping ratio ζ :

$$t_a = \begin{cases} \frac{1}{\omega_d} (3 \arctan \frac{\sqrt{1-\zeta^2}}{\zeta} - \pi), & 0 \leq \zeta \leq 0.5 \\ \frac{3}{\omega_d} \arctan \frac{\sqrt{1-\zeta^2}}{\zeta}, & 0.5 < \zeta < 1 \end{cases} \quad (11)$$

Substituting Equation (11) into Equation (9) yields the absolute value of the first extremum of the system acceleration response, which is:

$$|\ddot{x}(t_a)|_{\max} = \begin{cases} \omega_n e^{\frac{\zeta}{\sqrt{1-\zeta^2}}(\pi - 3 \arctan \frac{\sqrt{1-\zeta^2}}{\zeta})}, & 0 \leq \zeta \leq 0.5 \\ \omega_n e^{\frac{-3\zeta}{\sqrt{1-\zeta^2}} \arctan \frac{\sqrt{1-\zeta^2}}{\zeta}}, & 0.5 < \zeta < 1 \end{cases} \quad (12)$$

Substituting $t = 0$ into Equation (9) yields the absolute value of the acceleration response of the system at the beginning, which is:

$$|\ddot{x}(0)| = 2\omega_n \zeta \quad (13)$$

Figure 2 shows the relationship between the maximum acceleration response absolute value at the zero moment and the first extremum moment with the damping ratio.

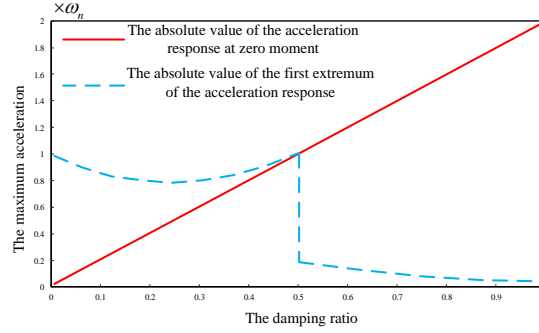


Figure 2. The relationship between the absolute maximum acceleration response and damping ratio

Figure 2 shows that, when $0 \leq \zeta \leq 0.5$, the absolute value of the acceleration response at the first extremum moment is greater than the acceleration at zero moment. In this case, the absolute value of the maximum acceleration response is $|\ddot{x}(t_a)|_{\max}$. However, when $0.5 < \zeta < 1$, the acceleration at time zero is greater than the absolute value of the acceleration response at the first extremum. In this case, the absolute value of the maximum acceleration response is $|\ddot{x}(0)|$.

In summary, the maximum value of the absolute value of the system acceleration response can be expressed as:

$$|\ddot{x}|_{\max} = \begin{cases} \omega_n e^{\frac{\zeta}{\sqrt{1-\zeta^2}}(\pi - 3 \arctan \frac{\sqrt{1-\zeta^2}}{\zeta})}, & 0 \leq \zeta \leq 0.5 \\ 2\omega_n \zeta, & 0.5 < \zeta < 1 \end{cases} \quad (14)$$

3.2. Steady-State Displacement Response Solution

From Equation (13), we can see that the time history of displacement response of the damping buffer system is shown in Figure 3. The dotted line in Figure 3 is the envelope line of displacement response.

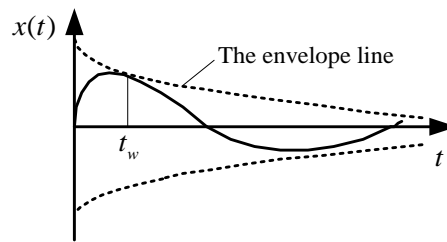


Figure 3. The time history of displacement response

In Figure 3, it can be seen that the envelope line function of the displacement response can be used to represent the steady-state displacement. The envelope line function equation is:

$$x_b(t) = \frac{1}{\omega_d} e^{-\zeta\omega_n t} \quad (15)$$

The absolute value of system steady-state displacement is:

$$|x_w| = \frac{1}{\omega_d} e^{-\zeta\omega_n t_w} \quad (16)$$

3.3. Recoil Displacement Response Solution

According to Equation (3), the system displacement response can be derived as:

$$x(t) = \frac{1}{\omega_d} e^{-\zeta\omega_n t} \sin \omega_d t = \frac{1}{\omega_n \sqrt{1-\zeta^2}} e^{-\zeta\omega_n t} \sin \omega_d t \quad (17)$$

Differentiating Equation (17) and setting the time derivative equal to zero, we can determine when the maximum displacement response happens, which gives:

$$t_x = \frac{1}{\omega_d} \left(\arctan \frac{\sqrt{1-\zeta^2}}{\zeta} + k\pi \right) \quad (18)$$

Since the displacement of the system at the beginning is zero, the time of the maximum value of the absolute value of the system displacement response is:

$$t_x = \frac{1}{\omega_d} \arctan \frac{\sqrt{1-\zeta^2}}{\zeta} \quad (19)$$

Substituting Equation (19) into Equation (17), the maximum value of the absolute value of the recoil displacement response can be obtained:

$$|x|_{\max} = \frac{1}{\omega_n} e^{\frac{-\zeta}{\sqrt{1-\zeta^2}} \arctan \frac{\sqrt{1-\zeta^2}}{\zeta}} \quad (20)$$

4. Parameter Optimization of Damping Buffer Device with Triple-Index Constraints

According to the range of different damping ratios, the optimization problem can be described by Equation (8):

When $0 \leq \zeta \leq 0.5$, the parameter optimization problems can be expressed as:

$$\left\{ \begin{array}{l} Q_1 = \min_{\omega_n, \zeta} \left| \omega_n e^{\frac{\zeta}{\sqrt{1-\zeta^2}} \left| \pi - 3 \arctan \frac{\sqrt{1-\zeta^2}}{\zeta} \right|} \right| \\ s.t. \\ \frac{1}{\omega_d} e^{-\zeta\omega_n t_w} < \sigma_{peak} \\ \frac{1}{\omega_n} e^{\frac{-\zeta}{\sqrt{1-\zeta^2}} \arctan \frac{\sqrt{1-\zeta^2}}{\zeta}} = X_{peak} \end{array} \right. \quad (21)$$

When $0.5 < \zeta < 1$, the parameter optimization problems can be expressed as:

$$\begin{cases} Q_1 = \min |2\omega_n \zeta| \\ s.t. \\ \frac{1}{\omega_d} e^{-\zeta \omega_n t_w} < \sigma_{peak} \\ \frac{1}{\omega_n} e^{\frac{-\zeta}{\sqrt{1-\zeta^2}} \arctan \frac{\sqrt{1-\zeta^2}}{\zeta}} = X_{peak} \end{cases} \quad (22)$$

If the maximum recoil displacement X_{peak} , the steady-state time t_w , and the maximum steady-state displacement σ_{peak} are provided, the minimum acceleration response Q_1 can be obtained based on Equations (21) and (22). Thus, the ω_n and ζ of the response are then determined to meet the design specifications for the natural frequency and damping ratio of the damping buffer device system accordingly. Lastly, the stiffness coefficient k and damping coefficient c of the system can be obtained.

It can be seen from the solution of the shock response in the previous section that there are contradictions in the selection of each parameter. The designed damping buffer device needs to meet three response requirements at the same time. However, the process of iterative solution using the conventional traversing method is not concise and effective. Thus, the following section discusses determining two parameters first, and then optimizing the another one.

4.1. ζ Solution at Maximum Acceleration and Recoil Displacement

Multiplying Equation (14) by Equation (20) yields:

$$|x|_{\max} |\ddot{x}|_{\max} = \begin{cases} e^{\frac{\zeta}{\sqrt{1-\zeta^2}} (\pi - 4 \arctan \frac{\sqrt{1-\zeta^2}}{\zeta})}, & 0 \leq \zeta \leq 0.5 \\ 2\zeta e^{\frac{-\zeta}{\sqrt{1-\zeta^2}} \arctan \frac{\sqrt{1-\zeta^2}}{\zeta}}, & 0.5 < \zeta < 1 \end{cases} \quad (23)$$

The constraint equation for the buffer system at maximum acceleration and recoil and its function curve are given in Equation (23) and Figure 4, respectively.

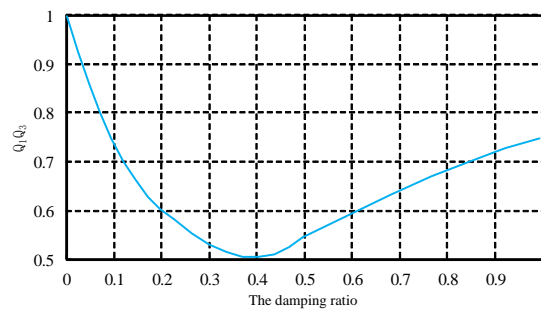


Figure 4. The relationship between the acceleration and recoil displacement are constrained by damping ratio

It can be seen from Figure 4 that an optimal ζ_{opt} , which is below 0.5, can be obtained at the maximum acceleration and recoil displacement. Furthermore, the value of ζ_{opt} is 0.404 based on Equation (21) when setting the derivative to zero. Note that ζ_{opt} is calculated considering the requirements for Q_1 and Q_3 only. The approach on how to satisfy the requirements for all three indexes will be provided in the next section.

4.2. Analysis of Relationship Between Q_2 and ζ at the Maximum Recoil Displacement

As shown in Equation (16) and Equation (20), there are no analytical expressions to derive Q_2 and Q_3 . The curve of recoil displacement constraint Q_2 will be changed with the change of the Q_3 value. The values of ω_n and ζ will be changed when the values of Q_2 and Q_3 are fixed. If the maximum recoil displacement is given, the curve of the relationship between Q_2 and ζ can be obtained by solving the optimization equation, which is shown in Figure 5.

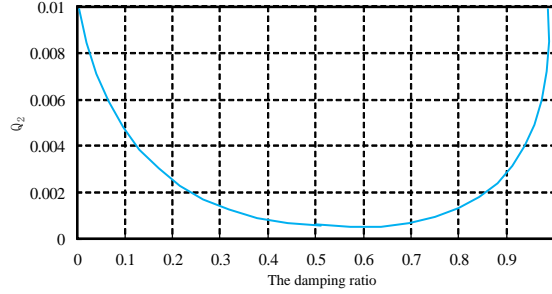


Figure 5. The relationship between steady-state displacement and damping ratio

As can be seen from Figure 5, it is possible for each steady-state displacement to obtain an effective damping ratio (at the minimum) at the maximum recoil displacement constraint, and it is also possible to obtain both damping ratios simultaneously. Therefore, the relationship between the other two indicators should be considered as well before making the choice.

4.3. Characteristic Parameters Solution at Constant Values of Three Indexes

Based on the analysis above, the process of solving the minimum acceleration index Q_1 at the maximum steady-state displacement index Q_2 and the maximum recoil displacement index Q_3 can be described as follows:

The range of ζ can be determined according to the given maximum steady-state displacement index Q_2 , while assuming the range of damping ratio (a, b).

The damping ratio at minimum acceleration response is then determined according to the values of a and b . As can be seen from Figure 2: when b is below 0.404, the minimum acceleration response Q_1 is obtained at the point $\zeta = b$; when a is over 0.404, the minimum acceleration response Q_1 is obtained at the point $\zeta = a$; however, when $a \leq 0.404 \leq b$, the minimum acceleration response Q_1 is obtained at the point $\zeta = 0.404$. Thus, the optimal damping ratio can be expressed as:

$$\zeta_{opt} = \begin{cases} b, & b < 0.404 \\ 0.404, & a \leq 0.404 \leq b \\ a, & 0.404 < a \end{cases} \quad (24)$$

The natural frequency ω_n can be obtained by introducing the optimal damping ratio ζ_{opt} into Equation (20). Assuming the maximum recoil displacement index is X_{peak} , then the natural frequency of the buffer system can be expressed as:

$$\omega_n = \frac{1}{X_{peak}} e^{\frac{-\zeta_{opt}}{\sqrt{1-\zeta_{opt}^2}} \arctan \frac{\sqrt{1-\zeta_{opt}^2}}{\zeta_{opt}}} \quad (25)$$

According to the first two steps to obtain ω_n and ζ_{opt} , the optimal stiffness coefficient k_{opt} and the optimal damping coefficient c_{opt} can be obtained based on ω_n and ζ_{opt} in the first two steps.

$$k_{opt} = m\omega_n^2 = \frac{m}{X_{peak}^2} e^{\frac{-2\zeta_{opt}}{\sqrt{1-\zeta_{opt}^2}} \arctan \frac{\sqrt{1-\zeta_{opt}^2}}{\zeta_{opt}}} \quad (26)$$

$$c_{opt} = 2\zeta_{opt} m\omega_n = \frac{2m\zeta_{opt}}{X_{peak}} e^{\frac{-\zeta_{opt}}{\sqrt{1-\zeta_{opt}^2}} \arctan \frac{\sqrt{1-\zeta_{opt}^2}}{\zeta_{opt}}} \quad (27)$$

These equations are derived and solved after normalization, so the step speed V_0 needs to be multiplied into those equations during the actual calculation. According to the law of momentum conservation, $V_0 = m_d v_0 / m_{hz}$, where m_d is the bullet mass, v_0 is the muzzle velocity of the bullet, and m_{hz} is the mass of the recoil portion.

5. Calculation and Analysis of Characteristic Parameters of Damping Buffer Device

In the existing program of the overhead 30-gun weapon station, the maximum recoil impact, maximum recoil displacement, and stable time are 48000N, 24.5mm, and 200ms, respectively. Firstly, the operation of this system will be more stable when the maximum recoil impact is reduced to below 40000N, according to the driving motor power, the requirements of the mounting system, and the viewing device for the permissible impact load. Secondly, the maximum firing rate of the overhead weapon station is 400rounds/min. In order to ensure that the recoil part can be quickly reset to the equilibrium position under automatic-firing condition, the stable time needs to be decreased to 150ms. This stable time is beneficial for improving the shooting accuracy. Besides, the existing feed mechanism limits the recoil displacement to 30mm. Thus, the maximum recoil displacement of the damping buffer device is set to 30mm.

In summary, the constraints of the damping buffer device at the overhead weapon station are as follows:

- the maximum recoil impact is less than 40000N;
- the stable time is less than 150ms;
- the maximum steady-state displacement is 2mm;
- the maximum recoil displacement is less than 30mm.

Some parameters of overhead weapon station are as follows: the mass of recoil part $m_{hz} = 282\text{kg}$, the bullet mass $m_d = 0.48\text{kg}$, and the muzzle velocity of the bullet $v_0 = 935\text{m/s}$. Then, substituting initial values and constraints above into the parameter optimization formula in the previous section, the optimal damping ratio can be obtained as $\zeta_{opt} = 0.607$. The $\omega_n = 52.6\text{rad/s}$ can be obtained by substituting ζ_{opt} into Equation (20). Moreover, the equations in this section are derived after normalization; hence, the calculation values need to be multiplied by the velocity step value $V_0 = m_d v_0 / m_{hz} = 1.6\text{m/s}$. $k = 780\text{N/mm}$ and $c = 18\text{N} \cdot \text{s/mm}$ can be obtained based on ζ_{opt} and ω_n .

In order to verify the effectiveness of the designed damping buffer device, k and c for the spring damping bumper are defined according to the design value in the rigid-flexible coupled dynamic model of the constructed overhead weapon station (as shown in Figure 6). Since two same springs are symmetrically arranged on both sides, the k and c values of the dynamic characteristics simulation are half of their theoretical values. Figure 7(a) and Figure 7(b) show the deformation curve and force curve of the damping buffer under the shooting condition. It can be seen that the maximum recoil force of the unilateral damping buffer received is 19852N. The maximum impact force of the recoil part is two times larger, which is less than 40000N. It meets the requirements of the indicator. Also, the maximum recoil displacement is 26.21mm and the stable time is 146ms, which means that they all satisfy the design requirements.

Figure 8 shows the acceleration at the centroid of the sights flange. It can be seen from the figure that the maximum impact acceleration of the sight device is reduced from 3014m/s^2 to 2257m/s^2 , which is 25.12%, after using the damping buffer device. The damping buffer device can effectively reduce the impact of the shooting load on the sighting device. Consequently, the sighting accuracy, tracking accuracy, and reliability of the sighting device during shooting can be further improved.

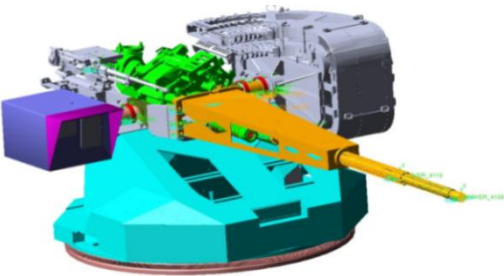


Figure 6. Rigid-flexible coupled dynamic model of overhead weapon station

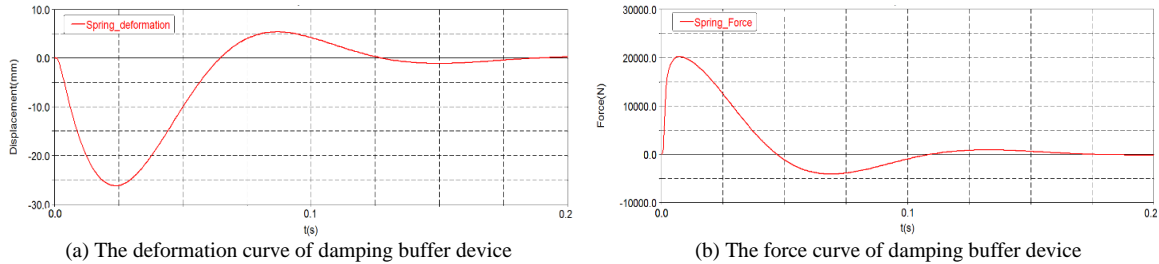


Figure 7. The curve of the damping buffer under shooting condition

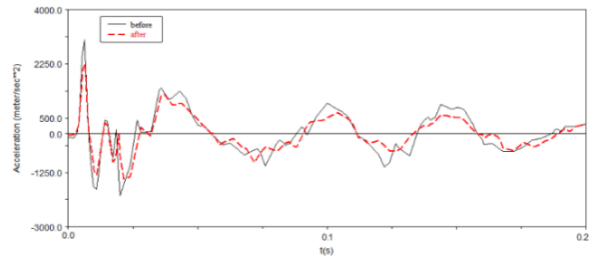


Figure 8. The comparison of impact acceleration curve of sighting device with damping buffer device

Figure 9(a) - Figure 9(d) show the comparison of the vibration parameters of the muzzle before and after using the damping buffer device. It can be seen from these figures that the peak values of the linear velocity and the angular displacement of the muzzle at the moment the bullet leaves the muzzle all are decreased. The angular displacement is decreased. Moreover, due to the increased damping, the vibration attenuation is significantly accelerated.

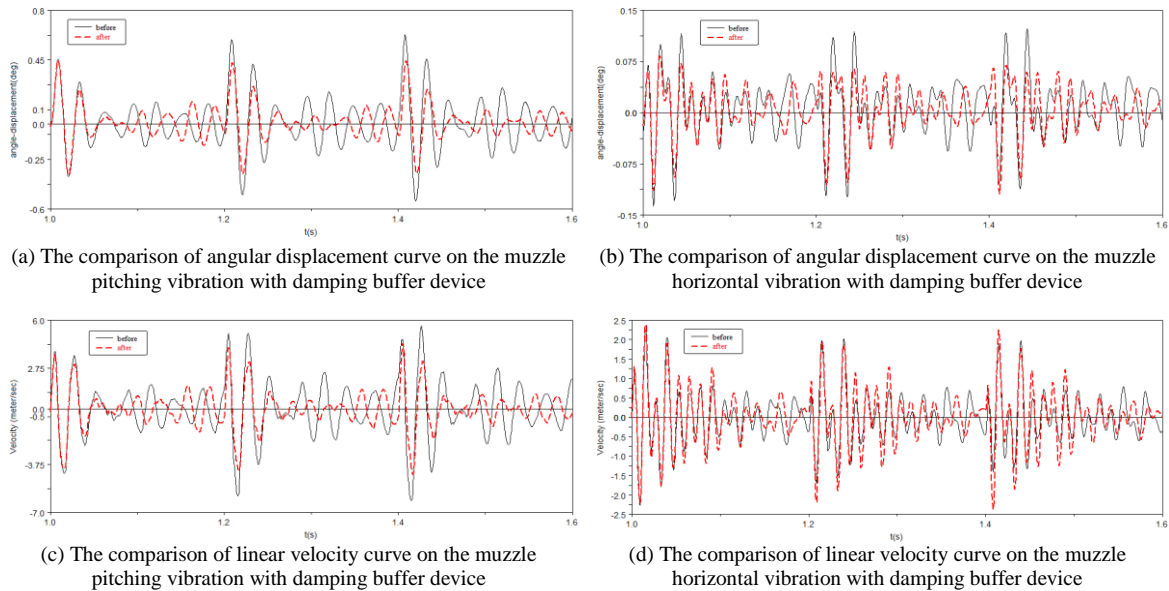


Figure 9. The characteristics of muzzle vibration with damping buffer device

Table 1 shows the comparison of vibration parameters variance before and after using the damping buffer device at the

moment the bullet leaves the muzzle. The dispersion variances are decreased after using the damping buffer device, among which the dispersion variance of pitching is reduced by 35.40% while the dispersion variance of horizontal is reduced by 30.77%.

Table 1. The comparison of vibration parameters variance with damping buffer device at the moment of bullet leaving the muzzle

	The variance of pitching angular displacement	The variance of horizontal angular displacement	The variance of pitching linear velocity
Without	0.000674	0.000073	0.066471
With	0.000467	0.000043	0.034728
Change rate/%	30.71	41.10	47.75
	The variance of horizontal linear velocity	The dispersion variance of pitching	The dispersion variance of horizontal
Without	0.010007	0.0113	0.0013
With	0.009139	0.0073	0.0009
Change rate/%	8.68	35.40	30.77

The damping buffer device on the overhead weapon station can greatly reduce the dispersion variance and therefore fundamentally reduce the recoil impact. This will also be beneficial for increasing the stability of the mounting system and the viewing device. Furthermore, the damping buffer device can be combined with the structural parameter optimization method in engineering practice. This approach will further improve the shooting accuracy and stability and promote the technology improvement for the overhead weapons station.

6. Conclusions

This paper proposed three indices to evaluate the performance of a recoil-attenuating device under real-world operating requirements, including the maximum acceleration, maximum steady-state displacement, and maximum recoil displacement. In addition, this paper also determined the system acceleration response, steady-state displacement response, and recoil displacement response with various damping ratios.

Through the optimization design analysis of the damping buffer device under the constraint of two indices, a method of solving the optimal buffer parameters under the constraint of three indices is proposed. Furthermore, the optimized stiffness of the damping buffer device is calculated as $k = 780 \text{ N/mm}$ and the optimized damping coefficient is calculated as $c = 18 \text{ N} \cdot \text{s/mm}$.

The optimized parameters of the damping buffer device are substituted into the model of an overhead weapon station for analysis. The results show that: (1) the maximum impact acceleration of the sighting device is reduced by 25.12%, which effectively reduces the recoil impact; (2) the dispersion variances of horizontal and pitching decreased by more than 30%, and thus the firing accuracy is greatly improved. In conclusion, the results can be used for the development of overhead weapon stations in the future.

References

1. B. Q. Mao, Y. L. Wu, Y. S. Gao, W. Dan, and F. Q. Lei, "A Summary for Vehicular Overhead Weapon Stations," *Journal of Academy of Armored Force Engineering*, Vol. 27, No. 5, pp. 1-7, May 2013
2. Y. Liang, J. R. Alvarado, K. D. Iagnemma, and A. E. Hosoi, "Dynamic Sealing Using Magneto-Rheological Fluids," *arXiv Preprint arXiv*, Vol. 1802, pp. 07912, 2018
3. A. Rossi, F. Orsini, A. Scorza, et al., "A Review on Parametric Dynamic Models of Magnetorheological Dampers and Their Characterization Methods," *Actuators, Multidisciplinary Digital Publishing Institute*, Vol. 7, No. 2, February 2018
4. B. S. M. Modrezejewski and S. Spears, "Rotating Shaft Damping with Electro-Rheological Fluid," *U.S. Patent 9*, Vol. 841, pp. 077, 2017
5. B. Titurus, J. D. Bois, N. Lieven, and R. Hansford, "A Method for the Identification of Hydraulic Damper Characteristics from Steady Velocity Inputs," *Mechanical Systems and Signal Processing*, Vol. 24, No. 8, pp. 2868-2887, August 2010
6. C. S. J. Chandra, P. K. Bipinbal, and K. N. Sunil, "Viscoelastic Behaviour of Silica Filled Natural Rubber Composites-Correlation of Shear with Elongational Testing," *Polymer Testing*, Vol. 60, pp. 187-197, 2017
7. B. Jiang, L. Q. Zhu, C. Z. Zhao, and Z. R. Chen, "An Investigation on the Bound Rubber and Dynamic Mechanical Properties of Polystyrene Particles-Filled Elastomer," *Polymer Composites*, Vol. 38, No. 6, pp. 1112-1117, June 2017
8. S. Nozaki, T. Hirai, Y. Higaki, K. Yoshinaga, and A. Takahara, "Effect of Chain Architecture of Polyol with Secondary Hydroxyl Group on Aggregation Structure and Mechanical Properties of Polyurethane Elastomer," *Polymer*, Vol. 116, pp. 423-428, 2017
9. H. J. Zhu, J. Yang, Y. Q. Zhang, and X. X. Feng, "A Novel Air Spring Dynamic Model with Pneumatic Thermodynamics, Effective Friction and Viscoelastic Damping," *Journal of Sound and Vibration*, Vol. 408, pp. 87-104, 2017

10. M. Ahmadian, R. J. Appleton, and J. A. Norris, "An Analytical Study of Fire Out of Battery Using Magneto-Rheological Dampers," *Shock and Vibration*, Vol. 9, pp. 129-142, 2002
11. M. Ahmadian, R. J. Appleton, and J. A. Norris, "Designing Magneto-Rheological Dampers in a Fire Out-of-Battery Recoil System," *IEEE Transactions on Magnetics*, Vol. 39, pp. 21-25, 2003
12. L. Jia, "Optimization Design of the New Metal Rubber Buffer on Artillery," Xi'an Technological University, Xi'an, 2013
13. S. R. Patil, S. Krishna, and S. S. Gawade, "Preparation, Characterization and Performance Analysis of BTO based High Yield Strength Electro-Rheological Fluid in Artillery Gun Recoil System Using FEA Approach," *Materials Today: Proceedings*, Vol. 5, No. 2, pp. 8222-8231, February 2018
14. S. Y. Chen, "Research on Damping Parameter Identification of Elastomer Buffer," Nanjing University, Nanjing, 2015
15. S. J. Shan and L. He, "Study on Error Source and Applicable Condition of Velocity Step Technique for Estimating Shock Response Amplitude," *Journal of Vibration and Shock*, Vol. 26, No. 1, pp. 90-95, January 2007
16. S. Z. Yang and K. C. Yang, "Basic Mechanic Engineering Control," Huazhong University of Science and Technology, Wuhan, 2000
17. X. J. Wu and S. J. Zhu, "Parameters Optimization of Shock Isolator Composed of Ordinary Components," *Journal of Vibration and Shock*, Vol. 24, No. 5, pp. 71-74, May 2005